DOI: 10.24352/UB.OVGU-2019-007 TECHNISCHE MECHANIK, 39, 1, (2019), 64 – 71
submitted: July 6, 2018

Energy Cascade in a Nonlinear Mechanistic Model of Turbulence

B. D. Bak, T. Kalmár-Nagy

Energy transfer plays an essential role in many natural and engineering processes which include different scales. Understanding how the energy cascade (which refers to the energy transfer among the different scales) works is of primary importance. One notable example is the energy cascade in turbulent flow whose kinetic energy is transferred from large eddies to smaller ones. Below a threshold scale the energy is dissipated due to viscous friction. We introduce a nonlinear phenomenological mechanistic model of turbulence which consists of masses connected by springs arranged in a binary tree structure. To represent the various scales, the masses are gradually decreased in lower levels. The bottom level of the model consists of nonlinear energy sinks to provide dissipation. Based on previous research, we choose the system parameters and analyze its behavior for simple impulsive excitations. The decay of the total mechanical energy and the discrete energy spectrum of the system are compared for different impulse magnitudes. It is demonstrated that the dissipation is much more significant compared to the linear model, if the input energy is large enough. The energy spectra are compared with that of the linear model. We find that the energy spectrum of the nonlinear model better highlights the cut-off feature of the Kolmogorov spectrum.

1 Introduction

There are many complex phenomena both in nature and in engineering processes which include energy transfer among a wide range of different scales. Many studies dealt with examining systems exhibiting energy cascades, see e.g. Vakakis et al. (2008). Frequently studied examples include nonlinear chain oscillators (Gendelman et al. (2001); Vakakis and Gendelman (2001)) and the Fermi-Pasta-Ulam problem described by Fermi et al. (1955). An energy cascade describes energy transfer primarily from large scales to small ones. There also exist inverse cascade models in which the energy is transferred from small scales to larger scales. A notable example is the forest fire model of Turcotte et al. (1999) which describes how small clusters of fires combine and form larger fires.

In fluid mechanics the well-known example of such a process is the turbulent energy cascade. According to Richardson (1922) there are vortices of different sizes in a turbulent flow. The larger vortices are unstable and break up to form several smaller vortices. Thus, the kinetic energy of the flow is transferred to smaller scales. The turbulent energy cascade is characterized by the energy spectrum $\hat{E}(\kappa)$ which shows the distribution of the total energy E of the flow among the different scales. In other words, the spectrum is a Fourier-transform of E, i.e.

$$E = \int \hat{E}(\kappa) d\kappa, \tag{1}$$

where the wavenumber $\kappa \sim 1/L$ is associated with the vortex having characteristic size L.

The spectrum of 3D homogeneous isotropic turbulence (also known as Kolmogorov spectrum, see Kolmogorov (1941)) is shown in Fig. 1.

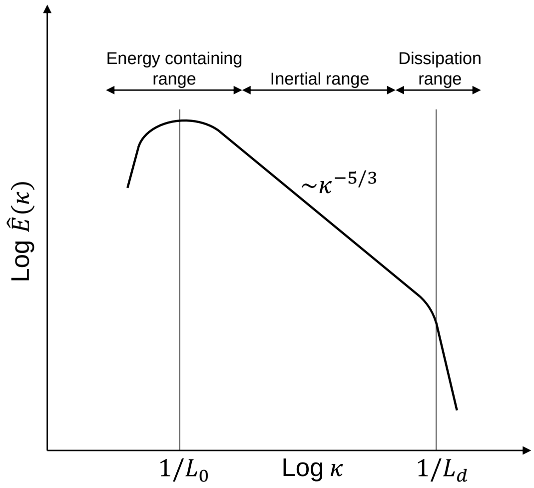

Figure 1: The Kolmogorov spectrum.

This spectrum corresponds to "pure turbulence": there are no force fields, boundary influences or any kind of disturbance. The flow statistics are spatially homogeneous and isotropic, temporally stationary or decaying. The energy spectrum shown in Fig. 1 describes the main features of the turbulent energy cascade. Energy production mainly affects the large scales (characterized by L_0), most of the energy is contained in the large eddies (energy containing range). There is an intermediate wavenumber range ($1/L_0 < \kappa < 1/L_d$) in which the energy spectrum is described by the scaling law

$$\hat{E}(\kappa) \sim \kappa^{-5/3}. \tag{2}$$

This part of the spectrum is called the inertial range. Dissipation becomes significant due to viscosity below the so called Kolmogorov length scale L_d. This is why the spectrum cuts off by large wavenumbers (dissipation range). A more detailed description of the Kolmogorov spectrum is given by Pope (2000).

The viability of the Kolmogorov spectrum was confirmed by means of both experimental and simulation techniques. For instance, various grid turbulence measurements are reported in the literature, e.g. Stalp et al. (1999); Kurian and Fransson (2009); Ertunç et al. (2010) and the results agree with Kolmogorov's notion of turbulence. Simulation tools are also extensively used to predict the statistics of turbulent flows, e.g. large eddy simulation was used by Kang et al. (2003), Galanti and Tsinober (2004) performed direct numerical simulations, Ditlevsen (2010) and Biferale (2003) reviewed the shell-models of turbulent energy cascade.

Our goal in this paper is to present a purely phenomenological model of turbulence which includes nonlinearity. Our mechanistic turbulence model is a binary tree of masses and springs (see Fig. 2), in which the masses represent the different scales, and the springs provide the connection among them. In a previous paper (Bak and Kalmár-Nagy (2018b)) we analyzed the response of a linear version of the system for impulsive and continuous harmonic excitations. We showed that among the scales of the linear system there is a qualitatively similar energy distribution as the Kolmogorov spectrum, if the model parameters are adequately chosen.

This paper is structured as follows: in Section 2 the phenomenological mechanistic model is described in details. In Section 3 we show how the energy dissipation depends on the input energy in the nonlinear mechanistic model. Furthermore, the energy spectrum of the model is described, and the characteristics of this spectrum is analyzed with different input energy levels. The energy spectra of the linear and nonlinear systems are compared. In Section 4 we draw conclusions. Throughout the analysis we consider every quantity to be dimensionless and/or normalized by a reference value.

2 Mechanistic Turbulence Model

2.1 Introduction of the Model

We introduce a mechanistic model of turbulence which is a binary tree of masses connected by springs. The tree has n levels, there are 2^{l-1} masses ($l = 1, ..., n$) in the lth level. The total number of masses is $N = 2^n - 1$. The model for $n = 3$ is depicted in Fig. 2.

The masses represent the different scales of vortices. The top mass (the largest vortex) is connected to the motionless ceiling with a spring. In the bottom level the masses (associated with the smallest, energy dissipating scale) are connected to the previous level with either linear or nonlinear springs and linear dampers.

In the nonlinear version of the model the parts responsible for the dissipation are nonlinear energy sinks (NES) as opposed to the linear model in which those are tuned mass dampers (TMD). Considering impulsive excitation, a fundamental difference between NES and TMD is that the effectiveness of the NES depends on the input energy magnitude, while the TMD is effective if it is tuned to the natural frequencies of the primary system. The behavior of a purely linear system is completely independent of the input energy magnitude.

Considering a system having at least 4 levels, the equations of motion for the masses in the different levels are

$$m_i \ddot{x}_i = \begin{cases} k_{2i}(x_{2i} - x_i) + k_{2i+1}(x_{2i+1} - x_i) - k_i x_i, \quad i = 1, \\ k_{2i}(x_{2i} - x_i) + k_{2i+1}(x_{2i+1} - x_i) - k_i(x_i - x_{\lfloor i/2 \rfloor}), \quad i = 2, ..., 2^{n-2} - 1, \\ k_{2i}(x_{2i} - x_i)^\beta + k_{2i+1}(x_{2i+1} - x_i)^\beta - k_i(x_i - x_{\lfloor i/2 \rfloor}) + \\ \qquad + c_{2i}(\dot{x}_{2i} - \dot{x}_i) + c_{2i+1}(\dot{x}_{2i+1} - \dot{x}_i), \quad i = 2^{n-2}, ..., 2^{n-1} - 1, \\ -k_i(x_i - x_{\lfloor i/2 \rfloor})^\beta - c_i(\dot{x}_i - \dot{x}_{\lfloor i/2 \rfloor}), \quad i = 2^{n-1}, ..., N. \end{cases} \tag{3}$$

The symbol $\lfloor . \rfloor$ denotes the floor operation. The exponent β=1 in the linear case and β=3 in the nonlinear case. The number of levels is $n \geq 4$.

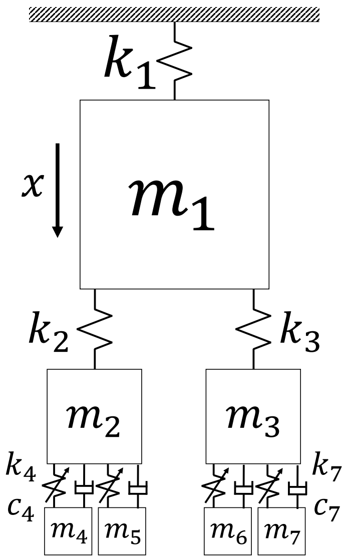

Figure 2: A 3-level mechanistic turbulence model.

2.2 Model Parameters

We set the masses, stiffnesses and dampers to be equal within a level. This allows us to introduce the following notations:

- M_l is the size of each mass in the lth level (i.e. $M_1 = m_1, M_2 = m_2 = m_3, ...$).
- K_1 denotes the stiffness of the top spring. K_l ($l = 2, ..., n$) denotes the stiffness coefficient of every spring which connects a mass of the $l-1$th and a mass of the lth levels.
- Every damper has the same damping coefficient which is denoted by C.

To represent the different length scales of vortices, the masses are gradually decreased in lower levels (a vortex of size L breaks up into smaller vortices). The power-law distribution

$$M_l = 1/2^{l-1}, \quad l = 1, ..., n, \tag{4}$$

specifies the masses in each level. Thus, the sum of masses in each level is 1, since $2^{l-1}M_l = 2^{l-1}(1/2)^{l-1} = 1$. Similarly to the masses, the K_l values are specified with a power-law distribution

$$K_l = \sigma^{l-1}, \quad \sigma > 0, \quad l = 1, ..., n, \tag{5}$$

whose single parameter is σ which is called the stiffness parameter. Thus, the stiffness of the top spring is $K_1 = \sigma^0 = 1$.

We define the damping ratio of the system as

$$\xi = C/2\sqrt{M_n K_n}. \tag{6}$$

The analysis of the previous linear model revealed that the energy spectrum (which we define in Section 3) in effect depends on σ, and is practically independent of ξ. In this paper we use $\xi = 0.001$, because such a weak damping well highlights how the nonlinear system behaves for different input energy magnitudes. Based on previous investigation of the linear model we set $\sigma = 0.45$, since for this σ the energy spectrum has many similarities with the Kolmogorov spectrum (see Bak and Kalmár-Nagy (2018b)). An 8-level system is analyzed for impulsive excitation. Every initial condition is set to zero, except $\dot{x}_1(0)$ (an initial velocity is set for the top mass).

3 Energy Transfer in the Mechanistic Model

3.1 The Total Mechanical Energy

The total mechanical energy $E(t)$ of the system is the sum of the kinetic energy stored in the masses, the potential energy stored in the linear springs, and the potential energy stored in the nonlinear springs, i.e.

$$E(t) = \frac{1}{2}\sum_{i=1}^{N} m_i\dot{x}_i^2 + \frac{1}{2}k_1 x_1 + \frac{1}{2}\sum_{i=2}^{2^{n-1}-1} k_i(x_i - x_{\lfloor i/2 \rfloor})^2 + \frac{1}{\beta+1}\sum_{i=2^{n-1}}^{N} k_i(x_i - x_{\lfloor i/2 \rfloor})^{\beta+1}. \tag{7}$$

The key difference between the linear and the nonlinear system is immediately seen from Fig. 3 which shows the percentage of $E(t)$ compared to the initial energy $E(0) = 1/2\dot{x}_1^2(0)$ for 8-level systems. In this figure the graph corresponding to the linear system ($\beta = 1$) is depicted with a solid line.

In the nonlinear system $E(t)$ strongly depends on the initial mechanical energy. For small $E(0)$ (see Fig. 3a) the dissipation is comparable to that of the linear system. As $E(0)$ increases, the dissipation becomes more significant (see Fig. 3b). This is in accordance with the description in Vakakis et al. (2008) which states that below a certain energy threshold the dissipation of the NES is not significant.

The evidence of a more efficient energy transfer realized by the NES compared to the TMD is shown in Fig. 4. In this figure $E_8(t)$ refers to the energy stored in the 8th level (the last level which includes the dissipating parts). Though the maximum percentage of $E_8(t)/E(t)$ is around 25% in both cases, there are much more spikes reaching this peak by the nonlinear case. The spikes are also wider in the nonlinear case. Thus, even for a moderately small impulse ($E(0) = 1$), more energy is transferred to the dissipating parts of the system in the same amount of time, if NESs are used instead of TMDs.

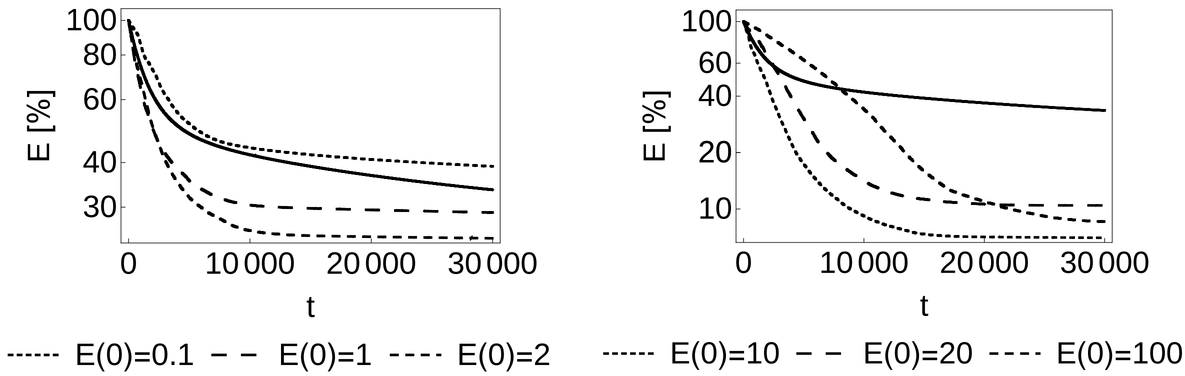

(a) Small input energy. (b) Large input energy.

Figure 3: The total mechanical energy of 8-level mechanistic models for different amount of initial energies. The continuous line corresponds to the linear system.

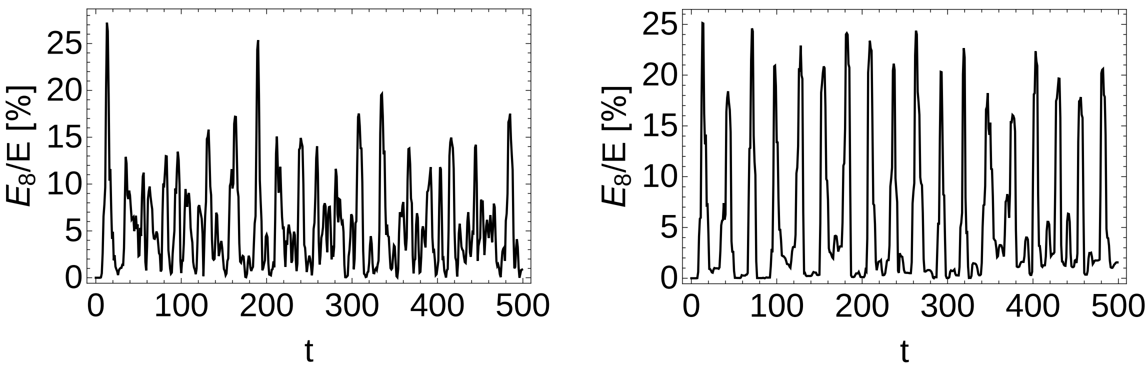

(a) Linear case. (b) Nonlinear case.

Figure 4: The percentage of the total mechanical energy of an 8-level system stored in the dissipating parts. The initial energy is $E(0) = 1$.

3.2 The Energy Spectrum

We compute $E_l(t)$ which is the mechanical energy stored in level l ($l = 1, ..., n$). Naturally, the kinetic energy of the masses located in level l contribute to $E_l(t)$. By design, the potential energy of the springs connecting two masses is distributed equally between the two levels. The potential energy of the top spring is added to $E_1(t)$. This definition of $E_l(t)$ ensures that $\sum_{l=1}^{n} E_l(t) = E(t)$, and $E_l(t) > 0$ for $t > 0$.

The mean total mechanical energy $\bar{E}$ of the system during the time period $[t_1, t_2]$ is $E(t)$ averaged over this time period, i.e.

$$\bar{E} = \frac{1}{t_2 - t_1} \int_{t_1}^{t_2} E(t) dt. \tag{8}$$

The mean mechanical energy $\bar{E}_l$ stored in level l can be calculated in the same manner, i.e.

$$\bar{E}_l = \frac{1}{t_2 - t_1} \int_{t_1}^{t_2} E_l(t) dt, \quad l = 1, ..., n. \tag{9}$$

In turbulent flow the energy spectrum $\hat{E}(\kappa)$ shows the "contribution" of the different scales to the total energy of the flow, i.e. the mean energy stored in the different wavenumbers κ (see Eq. (2)). Analogously to the wavenumber of a turbulent scale, we define the "wavenumber" of the masses in the lth level as

$$\kappa_l = 1/M_l, \quad l = 1, ..., n. \tag{10}$$

The energy fraction stored in wavenumber κ_l is defined as

$$\hat{E}_l(\kappa) = \bar{E}_l/\bar{E}, \quad l = 1, ..., n, \tag{11}$$

and it shows the “contribution” of a scale to the total mechanical energy of the system (each $\hat{E}_l(\kappa)$ belongs to a different “mass scale” M_l). The $\hat{E}_l(\kappa)$ values ($l = 1, ..., n$) constitute the discrete energy spectrum $\hat{E}(\kappa)$ of the mechanistic model.

Fig. 3 shows that the behavior of the system consists of an initial, highly dissipative part which is followed by a slowly decaying part. In the first part the spectrum heavily depends on the time interval $[t_1, t_2]$ (see Bak and Kalmár-Nagy (2018b)). In Bak and Kalmár-Nagy (2018a) we eliminated this dependence on the chosen time interval by calculating the spectrum of the linear system in the asymptotic limit of $t_1 \to \infty$. In practice we can approximate the spectrum corresponding to the asymptotic limit of $t_1 \to \infty$ by choosing a sufficiently large t_1. Therefore, in this study we extract the energy spectrum from $t \in [59900, 60000]$ for both the linear and nonlinear cases. Our experience is that the energy spectrum of the nonlinear system is also practically independent of the time interval $[t_1, t_2]$, if t_1 is sufficiently large. Typical energy spectra for different initial energies are shown in Fig. 5.

To make the comparison easier, the energy spectrum of the linear case ($\beta = 1$) is depicted in every plot. As Fig. 5 shows, the shape of the energy spectrum depends on the initial energy of the nonlinear system. In general, the cut-off at the largest wavenumber is much more significant in the nonlinear case.

For small initial energy (Fig. 5a) the slope of the spectrum of the nonlinear system is less steep than that of the linear system. The dissipative parts are very efficient for moderately large initial energy (Fig. 5b), and the cut-off at the largest wavenumber is less noticeable in this case. As the initial energy further increased (Fig. 5c) the spectrum of the nonlinear system becomes the same as that of the linear system, except at the largest wavenumber where the cut-off becomes significant again. Comparing Figs. 3 and 5 explains the more serious cut-off in the nonlinear cases. When the system is nonlinear, a plateau is observed in the plots of $E(t)$ after the initial, highly dissipative part. This means that the energy dissipation becomes insignificant. Thus, the energy fraction stored in the largest wavenumber (which corresponds to the dissipating nonlinear part) must be negligible, since otherwise the energy dissipation would be still significant. This is why a spectacular cut-off is present in the energy spectrum by the largest wavenumber. In the linear system the energy is still steadily decaying after the high initial dissipation, hence the cut-off in the energy spectrum is less significant.

Similarly to the Kolmogorov spectrum, the midrange of the energy spectra seemingly obeys a scaling law which is

$$\hat{E}(\kappa) \sim \kappa^{\alpha}, \tag{12}$$

where the scaling exponent α mainly depends on σ. In the nonlinear case α also depends on the input energy. For the linear model the scaling exponent $\alpha = -2.37$, while it is always larger or the same for the nonlinear model.

4 Conclusions

We analyzed a nonlinear mechanistic model of turbulence which is a binary tree of masses connected by springs. The bottom level of the system consists of NESs to model dissipation. The response of the system was studied for impulsive excitations which were applied to the top mass. These impulses had different magnitude to show that the behavior of the nonlinear system strongly depends on the input energy. We defined and showed the energy spectrum of the mechanistic model for linear and nonlinear cases. The parameters of the model (σ and ξ) were chosen to replicate an energy spectrum which is similar to the Kolmogorov spectrum. The choice was based on the analysis of the previously investigated linear model. Compared to the spectrum of the linear model, for small to moderate initial energy the spectrum of the nonlinear model contains more energy in the intermediate and large wavenumbers, except the largest wavenumber. At the largest wavenumber the spectrum cuts off. The cut-off is in general much more serious in the nonlinear case, because after the initially rapid energy dissipation the energy

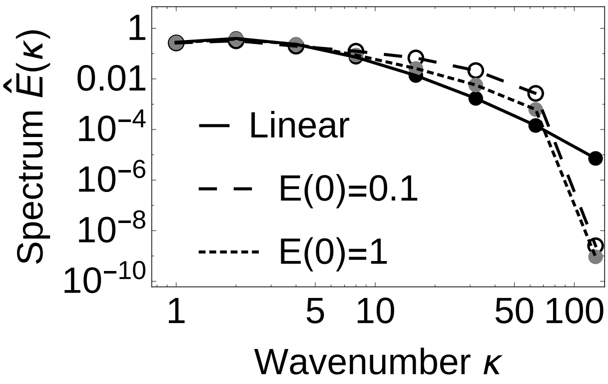

(a)

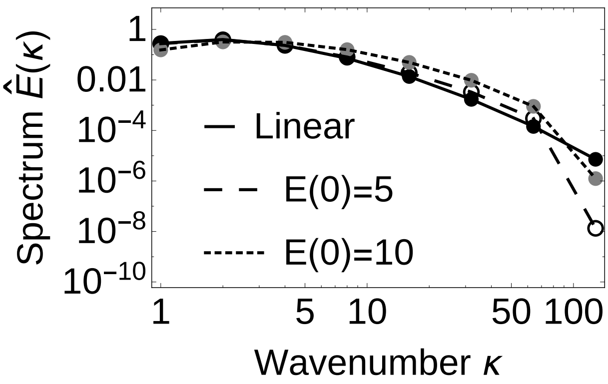

(b)

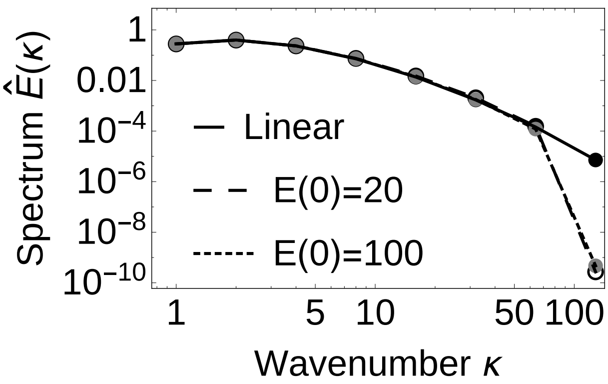

(c)

Figure 5: Energy spectra of the linear and nonlinear 8-level mechanistic models for different initial energies.

transfer to the dissipating bottom level becomes negligible. For large initial energy the spectra of the linear and the nonlinear cases are practically the same, except the largest wavenumber. Including nonlinearities in the model “improved” the shape of the spectrum in the sense that it better resembles the Kolmogorov spectrum with the more significant cut-off at the largest wavenumber. In future work we intend to include negative damping (which would correspond to internal energy generation) and more nonlinear springs at higher levels of the model to investigate the energy cascade of those systems.

Acknowledgements

This project was supported by the ÚNKP-17-3-I and ÚNKP-18-3-I New National Excellence Programs of the Ministry of Human Capacities of Hungary. We acknowledge the financial support from TeMA Talent Management Foundation. The research reported in this paper was supported by the Higher Education Excellence Program of the Ministry of Human Capacities in the frame of Water Science & Disaster Prevention research area of Budapest University of Technology and Economics (BME FIKP-VÍZ).

References

Bak, B. D.; Kalmár-Nagy, T.: Energy transfer in a linear turbulence model. In: *ASME 2018 International Design Engineering Technical Conferences and Computers and Information in Engineering Conference* (2018a), V006T09A038.

Bak, B. D.; Kalmár-Nagy, T.: A linear model of turbulence: reproducing the Kolmogorov-spectrum. *IFAC-PapersOnLine*, 51, 2, (2018b), 595–600.

Biferale, L.: Shell models of energy cascade in turbulence. *Annual Review of Fluid Mechanics*, 35, 1, (2003), 441–468.

Ditlevsen, P. D.: *Turbulence and shell models*. Cambridge University Press (2010).

Ertunç, Ö.; Özyilmaz, N.; Lienhart, H.; Durst, F.; Beronov, K.: Homogeneity of turbulence generated by static-grid structures. *Journal of Fluid Mechanics*, 654, (2010), 473–500.

Fermi, I.; Pasta, P.; Ulam, S.; Tsingou, M.: Studies of the nonlinear problems. Tech. rep., Los Alamos Scientific Lab., New Mexico (1955).

Galanti, B.; Tsinober, A.: Is turbulence ergodic? *Physics Letters A*, 330, 3, (2004), 173–180.

Gendelman, O.; Manevitch, L.; Vakakis, A. F.; M'closkey, R.: Energy pumping in nonlinear mechanical oscillators: Part I-dynamics of the underlying hamiltonian systems. *Journal of Applied Mechanics*, 68, 1, (2001), 34–41.

Kang, H. S.; Chester, S.; Meneveau, C.: Decaying turbulence in an active-grid-generated flow and comparisons with large-eddy simulation. *Journal of Fluid Mechanics*, 480, (2003), 129–160.

Kolmogorov, A. N.: The local structure of turbulence in incompressible viscous fluid for very large Reynolds numbers. In: *Dokl. Akad. Nauk SSSR*, vol. 30, pages 301–305, JSTOR (1941).

Kurian, T.; Fransson, J. H. M.: Grid-generated turbulence revisited. *Fluid Dynamics Research*, 41, 2, (2009), 021403.

Pope, S. B.: *Turbulent Flows*. Cambridge University Press (2000).

Richardson, L. F.: *Weather Prediction by Numerical Process*. Cambridge University Press (1922).

Stalp, S. R.; Skrbek, L.; Donnelly, R. J.: Decay of grid turbulence in a finite channel. *Physical Review Letters*, 82, 24, (1999), 4831.

Turcotte, D.; Malamud, B.; Morein, G.; Newman, W.: An inverse-cascade model for self-organized critical behavior. *Physica A: Statistical Mechanics and its Applications*, 268, 3-4, (1999), 629–643.

Vakakis, A. F.; Gendelman, O.: Energy pumping in nonlinear mechanical oscillators: part II-resonance capture. *Journal of Applied Mechanics*, 68, 1, (2001), 42–48.

Vakakis, A. F.; Gendelman, O. V.; Bergman, L. A.; McFarland, D. M.; Kerschen, G.; Lee, Y. S.: *Nonlinear Targeted Energy Transfer in Mechanical and Structural Systems*, vol. 156. Springer Science & Business Media (2008).

Address: Department of Fluid Mechanics, Faculty of Mechanical Engineering, Budapest University of Technology and Economics. Bertalan Lajos u. 4 - 6, H-1111 Budapest, Hungary.
email: `bak@ara.bme.hu, kalmarnagy@ara.bme.hu`